

Cite this: *Phys. Chem. Chem. Phys.*,
2014, 16, 5774

Photoexcited carrier dynamics of double-layered CdS/CdSe quantum dot sensitized solar cells measured by heterodyne transient grating and transient absorption methods

N. Osada,^{ab} T. Oshima,^b S. Kuwahara,^a T. Toyoda,^{bc} Q. Shen^{*bc} and K. Katayama^{*a}

The charge dynamics in the double-layered quantum dot sensitized solar cell (QDSSC) was studied to clarify the reason why the cell performance was much improved by a double-layer coating, by using the heterodyne transient grating (HD-TG) and transient absorption methods, based on a previous study for a conventional QDSSC (N. Maeda *et al.*, *Phys. Chem. Chem. Phys.*, 2013, **15**, 11006.) In the double-layered QDSSC, the layer order of CdS and CdSe affected the cell performance. When CdS is in between TiO₂ and CdSe, the conversion efficiency was enhanced by 70%, while it was lowered by 50% in the opposite order. From the information on charge dynamics, it was found that electrons were efficiently injected to TiO₂ by appropriate band alignment of CdS and CdSe, while only a part of the electrons were transferred to the TiO₂ when the layer order was opposite. Furthermore, the reverse electron transfer does not matter for the conversion efficiency, because the process increased even for the appropriate layer order.

Received 9th December 2013,
Accepted 8th January 2014

DOI: 10.1039/c3cp55177f

www.rsc.org/pccp

Introduction

In the last ten years, the conversion efficiency of quantum dot sensitized solar cells (QDSSCs) showed drastic improvement. QD have properties appropriate for light harvesting applications such as tunable optical absorption by size control and high efficiency multiple exciton generation (MEG).^{1–3} The theoretical efficiency is as high as 44%, higher than that for dye-sensitized solar cells (DSSCs).⁴ Furthermore, from a manufacturing viewpoint, the production cost is expected to be much cheaper due to abundant inorganic materials. However, the conversion efficiency at the moment is still lower than that for DSSCs,^{5–7} although it has been greatly improved in the last few years to nearly 7%,^{8,9} and much efforts have been made on the QD size,^{10,11} the core–shell structure of QDs,^{9,12} surface fabrication and passivation,^{11,13,14} and semiconductors and substrates,^{6,15,16} and their optimal combinations.¹⁷

As a promising effort, mixing of different kinds of QDs as a sensitizer has been reported in recent years. It was first reported by Hodes *et al.*, and the composition of the QD layer

was studied carefully.¹⁸ The blend of QDs helps the electrons flow smoothly by tuning the band position alignment^{19,20} and also expanding the absorption wavelength region for light harvesting. Lee *et al.*²⁰ clarified by ultraviolet photoelectron spectroscopy that the band position of CdSe shifted upwards when a CdS layer was in-between TiO₂ and CdSe. The charge transfer between the CdS/CdSe QDs and TiO₂ was studied by photoluminescence dynamics, which indicated smooth charge transfer by co-sensitizing CdS and CdSe on TiO₂.²¹ This blend electrode was also used for sensitization of nanotubes,^{22–24} and hierarchical TiO₂²⁵ for hydrogen evolution at the counter electrode.¹⁹ Recently, Zhong *et al.* prepared a well-ordered core–shell structure of CdS–CdSe QDs and reached 5.32% conversion efficiency,¹² and Kamat *et al.* demonstrated a Mn-doped CdS/CdSe QDSSC and reached 5.42% efficiency.²⁶ The long-lived exciton for CdSe/CdS QDs was studied from a fundamental viewpoint for utilization of photoexcited carriers.^{27,28}

There is another approach for improving the conversion efficiency, by understanding the mechanism of charge dynamics, typically by using the transient absorption (TA) method. The materials or their combination were modified based on the mechanism information to enhance the injection efficiency and to reduce recombination probabilities. In this field, Hodes *et al.*²⁹ reviewed the charge processes as compared to those for DSSCs and Kamat *et al.*^{1,10,30} studied the initial charge injection process by the TA method and explained it with the Gibbs energy of the QDs and the conduction band of

^a Department of Applied Chemistry, Chuo University, 1-13-27, Kasuga, Bunkyo, Tokyo 112-8551, Japan. E-mail: kkata@kc.chuo-u.ac.jp; Fax: +81-3-3817-1913; Tel: +81-3-3817-1913

^b Department of Engineering Science, The University of Electro-Communications, 1-4-1 Chofugaoka, Chofu, Tokyo 182-8585, Japan. E-mail: shen@pc.uec.ac.jp

^c CREST, Japan Science and Technology Agency (JST), 4-1-8 Honcho Kawaguchi, Saitama 332-0012, Japan



the semiconductor; Shen and Gomez *et al.*,^{31–33} studied not only electron but also hole dynamics on the order of picoseconds, which clarified the hole transfer to the electrolyte species.

On the other hand, we have developed a combination methodology of heterodyne transient grating (HD-TG), TA, and transient photocurrent (TP) methods measured in a wide time range from nanoseconds to seconds, and we have studied the charge carrier dynamic in DSSCs³⁴ and QDSSCs³⁵ to improve the conversion efficiency. The difference of our methodology is that we could monitor not only the electrons or holes on the electrode side, but also the dynamics of the redox or electrolyte species on the liquid side at the interface. This is possible because the HD-TG technique we have developed measures the refractive index change, which is very sensitive to dipole change, and thus the charged species at the interface was sensitively monitored. By combination with the TA method, we could get the whole information on charge carriers in the solid, interface, liquid side.

In a previous paper, we showed the dependence on pump intensity, applied bias, electrolyte, for the CdSe QDSSC, and the observed dynamics was assigned from the nanosecond to second order. Furthermore, the effect of ZnS coating was investigated, and optimal coating conditions were proposed by observation of the electron/electrolyte recombination and electron dynamics in TiO_2 .³⁵ In this study, we studied the charge dynamics in CdSe/CdS QDSSCs, and clarified why the conversion efficiency was improved by double-layer coating.

Experimental

The method for preparation of the working electrodes was reported in a previous paper.³⁶ Anatase TiO_2 paste was prepared by mixing TiO_2 nanoparticles with an average diameter of 15 nm (3.0 g), polyethylene glycol with molecular weight of 500 000 (1.2 g), acetyl acetone (1.0 mL) and water (10 mL) with a mortar for 30 min. The resulting paste was cast onto a glass substrate coated with fluorine doped tin oxide (FTO, 10 Ω , Asahi Glass) with a Scotch tape as a frame and spacer, raking off the excess solution with a glass rod. (Squeegee technique) The TiO_2 electrodes were dried in air at room temperature for 10 min, and annealed at 450 °C for 30 min in a furnace, and then cooled down to rt. The film thickness was around $7 \pm 1 \mu\text{m}$.

CdS ³⁷ and CdSe ³⁸ were grown with the chemical bath deposition (CBD) method. A TiO_2 electrode was immersed in a mixture solution of CdCl_2 (20 mM), NH_4Cl (66 mM), NH_3 (230 mM), H_2NCSNH_2 (140 mM) for 40 min for the CdS QDs deposition. For the CdSe QDs deposition, an electrode was immersed in a mixture of CdSO_4 (27 mM), $\text{N}(\text{CH}_2\text{COONa})_3$ (40 mM), Na_2SeSO_3 (27 mM) solution. A TiO_2 electrode with CdS QDs was immersed for 6 h, and a bare TiO_2 electrode was immersed for 24 h. Zinc sulfide (ZnS) was coated by the SILAR method.³⁹ The electrodes were soaked in $(\text{CH}_3\text{COO})_2\text{Zn}$ (0.1 M) and Na_2S (0.1 M) solutions in turns with two cycles. A polysulfide solution was used as electrolyte solution with S and Na_2S concentrations of 1 M.⁴⁰ Cu_2S was used as a counter electrode.

The principle and the setup of the HD-TG method were reported in detail in previous papers.^{34,41,42} In this study, the pump light source was an OPO (Surelite II – 10FP) output excited by a Nd:YAG laser (Panther, Continuum, Electro-Optics Inc.), and the pulse light had a wavelength of 570 nm, a pulse width of 5 ns, and a repetition rate of 0.5 Hz. The repetition rate was decided upon as being slow enough to recover the original baseline for the HD-TG and TA measurements. The pump intensity was 0.65 mJ per pulse. The probe light was a fiber coupled CW semiconductor laser with a wavelength of 658 nm for all HD-TG (10 mW) and TA measurements (4 mW). The pump and probe lights were incident from the FTO substrate side to avoid absorption of the pump light by polysulfide redox solution. TA responses were measured at the same probe wavelength just by removing a glass plate of transmission grating used for the HD-TG measurement.

The photoacoustic (PA) spectrum was measured with a home-built apparatus, and the measured wavelength range was 270–900 nm.⁴³ The $I\text{-}V$ curves were measured under A.M.1.5 for the area of 0.24 cm^2 by a solar simulator (Peccell:PEC-L10). IPCE was measured using home-built IPCE equipment (0.8–1 mW cm^{-2} for monochromic light).

Results and discussions

We prepared different types of electrodes, TiO_2 only, CdSe/TiO_2 , CdS/TiO_2 , $\text{CdSe}/\text{CdS}/\text{TiO}_2$, $\text{CdS}/\text{CdSe}/\text{TiO}_2$ electrodes. To confirm the growth of QDs and the band gap energy for the electrodes, PA spectra were measured for them, and the results are shown in Fig. 1. As we expected, the absorption region was extended to 1.75 eV for the CdSe/TiO_2 , $\text{CdSe}/\text{CdS}/\text{TiO}_2$, $\text{CdS}/\text{CdSe}/\text{TiO}_2$ electrodes mostly due to the absorption of CdSe QDs and no difference was observed for the three electrodes. A small absorption increase was observed for the CdS/TiO_2 electrode as compared to the TiO_2 only electrode. Based on the effective mass approximation, the average size of CdSe QDs was 7 nm. (Bulk band gap: 1.75 eV, electron and hole mass: 1.18×10^{-31} and 4×10^{-31} kg for CdSe were used.)⁴⁴

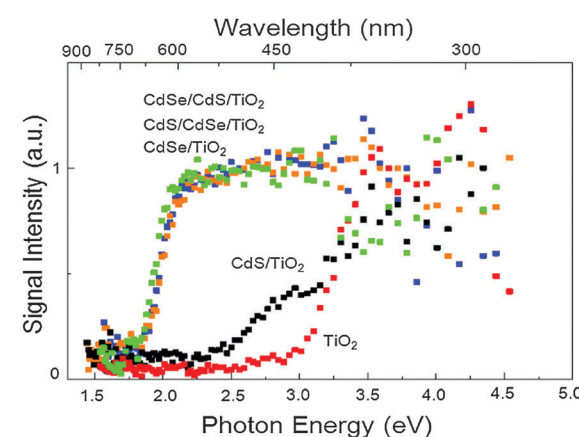


Fig. 1 PA spectra for the electrodes; TiO_2 only, CdSe/TiO_2 , CdS/TiO_2 , $\text{CdSe}/\text{CdS}/\text{TiO}_2$, $\text{CdS}/\text{CdSe}/\text{TiO}_2$ electrodes.

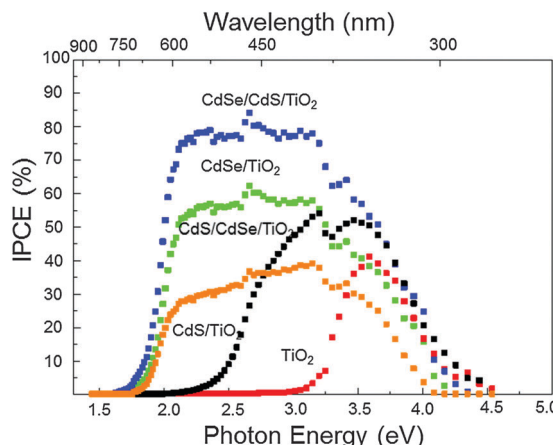
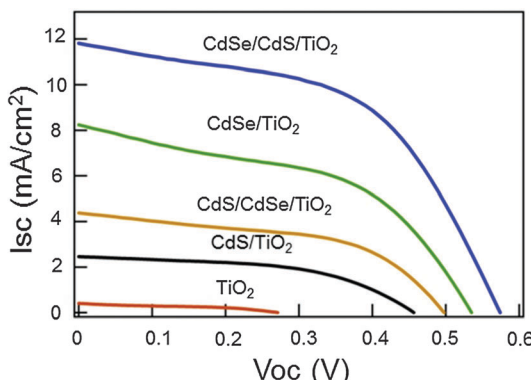


Fig. 2 IPCE spectra for the electrodes; TiO_2 only, CdSe/TiO_2 , CdS/TiO_2 , $\text{CdSe}/\text{CdS}/\text{TiO}_2$, $\text{CdS}/\text{CdSe}/\text{TiO}_2$ electrodes.

Next, IPCE was measured for the electrodes (Fig. 2). As we expected, the energy range was extended only to 2.2 eV for the CdS/TiO_2 electrode. The energy regions of the IPCE for the CdSe/TiO_2 , $\text{CdSe}/\text{CdS}/\text{TiO}_2$, $\text{CdS}/\text{CdSe}/\text{TiO}_2$ electrodes were similar, but IPCE intensity was drastically changed by the presence and the layer order of CdS and CdSe. When the CdS layer was in between TiO_2 and CdSe, IPCE was enhanced by about 30% as compared to the CdSe/TiO_2 electrode, while it was lowered by about 40% when the CdS layer was on top of the electrode.

The I - V curves for the electrodes were measured and the result is shown in Fig. 3. Similar to the IPCE result, the I - V characteristic was slightly improved in the presence of CdS QDs as compared to a bare TiO_2 electrode, and considerably improved in the presence of CdSe QDs, reaching a conversion efficiency of 2.1%. By mixing the CdS and CdSe, the result was influenced by



QDs	I_{sc} (mA/cm^2)	V_{oc} (V)	FF(-)	η (%)
CdSe/TiO_2	8.2	0.54	0.48	2.1
$\text{CdSe}/\text{CdS}/\text{TiO}_2$	11.9	0.58	0.52	3.6
$\text{CdS}/\text{CdSe}/\text{TiO}_2$	4.4	0.50	0.51	1.1
CdS/TiO_2	2.5	0.46	0.51	0.58
TiO_2 only	0.41	0.27	0.40	0.044

Fig. 3 I - V curves for the electrodes; TiO_2 only, CdSe/TiO_2 , CdS/TiO_2 , $\text{CdSe}/\text{CdS}/\text{TiO}_2$, $\text{CdS}/\text{CdSe}/\text{TiO}_2$ electrodes, and their I - V characteristics.

the order of CdS and CdSe coating. When the CdS QDs were in between CdSe and TiO_2 , both the J_{sc} and V_{oc} were improved, and the conversion efficiency was improved by 70% as compared to the CdSe only, while the opposite tendency was observed when the CdS QDs were on top of the layer, and the efficiency became almost half of the CdSe only.

To study how the combination of CdSe and CdS affected the conversion efficiency, we studied the charge dynamics by TA and HD-TG measurements. The pump wavelength for these measurements was selected at 570 nm to selectively excite the CdSe QDs.

The TA responses for the CdSe/TiO_2 , $\text{CdSe}/\text{CdS}/\text{TiO}_2$, $\text{CdS}/\text{CdSe}/\text{TiO}_2$ electrodes are shown in Fig. 4. As we have already assigned, the dynamics consisted of the decay of trapped electrons in TiO_2 in the 1–100 ms region and the long lasting decay from μs –100 ms corresponding to the inhomogeneously distributed conduction electrons in TiO_2 .^{35,45} For the $\text{CdSe}/\text{CdS}/\text{TiO}_2$ electrode, the trapped electrons were considerably increased as compared to the CdSe/TiO_2 electrode, while they decreased for the $\text{CdS}/\text{CdSe}/\text{TiO}_2$ electrode. It means that the electrons were effectively accumulated in TiO_2 for the former electrode, but they were lost for the latter one.

Next, HD-TG measurements were performed for the CdSe/TiO_2 , $\text{CdSe}/\text{CdS}/\text{TiO}_2$, $\text{CdS}/\text{CdSe}/\text{TiO}_2$ electrodes (Fig. 5). In the HD-TG responses for a QDSSC electrode, we can observe reorganization of the ionic species at the interface in 1–100 μs , a thermal response in 0.1–1 ms, and reverse electron transfer to redox species in 1–100 ms.³⁵ Since the thermal response does not matter in the process of charge dynamics, the 1st and 3rd components were considered. A scheme corresponding to the band alignment of CdSe, CdS and TiO_2 is shown in Scheme 1 to understand the charge dynamics.^{19,20} As compared to the CdSe/TiO_2 electrode, the 1st component was delayed and the 3rd component increased a little in its intensity for the $\text{CdSe}/\text{CdS}/\text{TiO}_2$ electrode. In the case of the $\text{CdS}/\text{CdSe}/\text{TiO}_2$ electrode, the 1st component was delayed and the 3rd component completely disappeared. It was unexpected because the electrode with lower conversion efficiency showed a smaller amount of the electrons

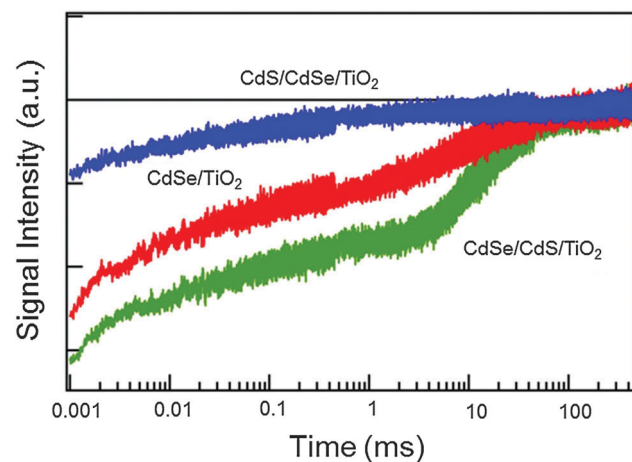


Fig. 4 TA responses for CdSe/TiO_2 , $\text{CdSe}/\text{CdS}/\text{TiO}_2$, $\text{CdS}/\text{CdSe}/\text{TiO}_2$ electrodes. The pump wavelength was 570 nm.



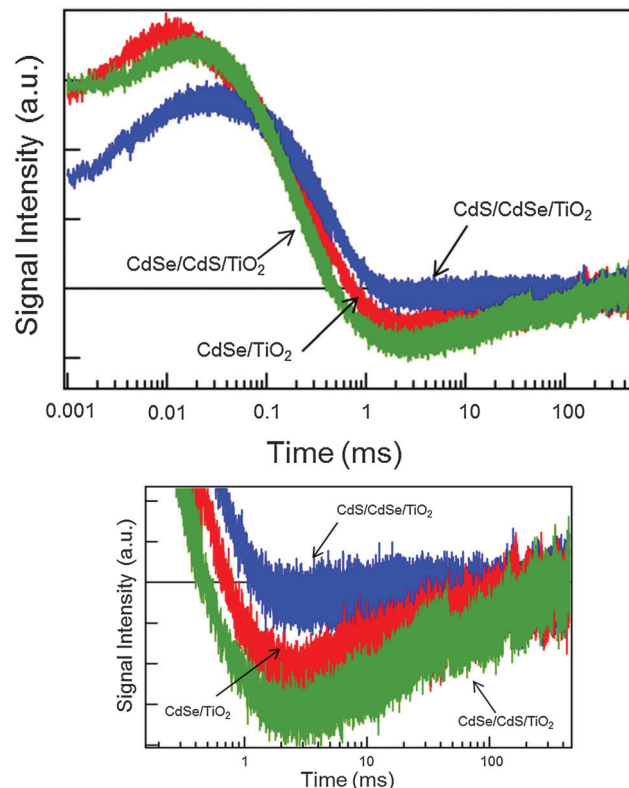
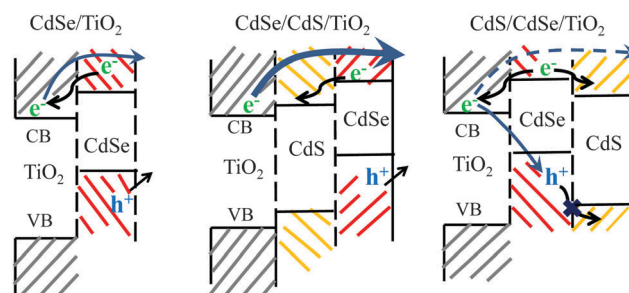


Fig. 5 HD-TG responses for the CdSe/TiO₂, CdSe/CdS/TiO₂, CdS/CdSe/TiO₂ electrodes. The pump wavelength was 570 nm. The bottom figure is the expansion in the 1–100 ms range.



Scheme 1 Band alignment of CdSe/TiO₂, CdSe/CdS/TiO₂, CdS/CdSe/TiO₂ electrodes. The arrow from the TiO₂ conduction band indicates back electron transfer or recombination processes.

which were subject to reverse electron transfer. For the CdSe/CdS/TiO₂ electrode, it is considered that the electrons were efficiently injected into TiO₂, which was supported by the fact of the increase in the accumulated electrons in TiO₂ from the TA result, and that more electrons were subject to reverse electron transfer. For the CdS/CdSe/TiO₂ electrode, based on Scheme 1, this can be explained with two possible reasons; (1) the band alignment suggests that only a part of the electrons were injected into TiO₂, while the other part of the electrons moved to the CdS side. The TA result supports the decrease in the amount of accumulated electrons into TiO₂. The amount of reverse electron transfer was decreased because of the decrease in the accumulated electrons in TiO₂. (2) The generated holes in

CdSe were difficult to move to the CdS side because of the energy barrier, and the holes were confined in the CdSe layer. The higher density of the holes in CdSe caused recombination with the electrons in TiO₂. It is likely that the second reason would be true because, if the 1st reason were true, some part of the electrons would still be subjected to the reverse electron transfer process, which would give some signal intensity for the 3rd HD-TG component. For both electrodes, the 1st component was delayed because the double semiconductor layers screened effectively the Coulomb force of the electrons in TiO₂, which caused the motion of ionic species to slow down.

Conclusions

We could confirm improvement of the QDSSCs by using the double layer of CdSe and CdS QDs, and the order of the coating was important; only when the CdS layer was in-between the TiO₂ and CdSe QDs, the IPCE, the *I*-*V* characteristic and the conversion efficiency were improved, while they decreased when the CdS layer was on the top of the electrode. This reason was studied with charge dynamics measurements and TA and HD-TG methods. It was clarified that due to the appropriate band alignment for the CdSe/CdS/TiO₂ electrode, the injected electrons were smoothly transferred to TiO₂ and accumulated there, and reverse electron transfer did not matter for the efficiency.

References

- 1 P. V. Kamat, *J. Phys. Chem. C*, 2008, **112**, 18737–18753.
- 2 S. Ruhle, M. Shalom and A. Zaban, *ChemPhysChem*, 2010, **11**, 2290–2304.
- 3 Q. Shen, K. Katayama, T. Sawada, S. Hachiya and T. Toyoda, *Chem. Phys. Lett.*, 2012, **542**, 89–93.
- 4 M. C. Hanna and A. J. Nozik, *J. Appl. Phys.*, 2006, **100**, 074510–074518.
- 5 Q. X. Zhang, X. Z. Guo, X. M. Huang, S. Q. Huang, D. M. Li, Y. H. Luo, Q. Shen, T. Toyoda and Q. B. Meng, *Phys. Chem. Chem. Phys.*, 2011, **13**, 4659–4667.
- 6 S. Q. Huang, Q. X. Zhang, X. M. Huang, X. Z. Guo, M. H. Deng, D. M. Li, Y. H. Luo, Q. Shen, T. Toyoda and Q. B. Meng, *Nanotechnology*, 2010, **21**, 1–7.
- 7 Q. Shen, A. Yamada, S. Tamura and T. Toyoda, *Appl. Phys. Lett.*, 2010, **97**, 123107.
- 8 Z. Pan, K. Zhao, J. Wang, H. Zhang, Y. Feng and X. Zhong, *ACS Nano*, 2013, **7**, 5215–5222.
- 9 J. Wang, I. Mora-Seró, Z. Pan, K. Zhao, H. Zhang, Y. Feng, G. Yang, X. Zhong and J. Bisquert, *J. Am. Chem. Soc.*, 2013, **135**, 15913–15922.
- 10 I. Robel, M. Kuno and P. V. Kamat, *J. Am. Chem. Soc.*, 2007, **129**, 4136–4137.
- 11 H. Zhang, K. Cheng, Y. M. Hou, Z. Fang, Z. X. Pan, W. J. Wu, J. L. Hua and X. H. Zhong, *Chem. Commun.*, 2012, **48**, 11235–11237.
- 12 Z. Pan, H. Zhang, K. Cheng, Y. Hou, J. Hua and X. Zhong, *ACS Nano*, 2012, **6**, 3982–3991.



13 I. Mora-Sero, S. Gimenez, F. Fabregat-Santiago, R. Gomez, Q. Shen, T. Toyoda and J. Bisquert, *Acc. Chem. Res.*, 2009, **42**, 1848–1857.

14 T. Toyoda and Q. Shen, *J. Phys. Chem. Lett.*, 2012, **3**, 1885–1893.

15 L. J. Diguna, Q. Shen, J. Kobayashi and T. Toyoda, *Appl. Phys. Lett.*, 2007, **91**, 023116.

16 M. Samadpour, S. Gimenez, P. P. Boix, Q. Shen, M. E. Calvo, N. Taghavinia, A. I. Zad, T. Toyoda, H. Miguez and I. Mora-Sero, *Electrochim. Acta*, 2012, **75**, 139–147.

17 I. Mora-Sero, S. Gimenez, F. Fabregat-Santiago, R. Gomez, Q. Shen, T. Toyoda and J. Bisquert, *Acc. Chem. Res.*, 2009, **42**, 1848–1857.

18 O. Niitsoo, S. K. Sarkar, C. Pejoux, S. Rühle, D. Cahen and G. Hodes, *J. Photochem. Photobiol. A*, 2006, **181**, 306–313.

19 Y.-L. Lee, C.-F. Chi and S.-Y. Liau, *Chem. Mater.*, 2009, **22**, 922–927.

20 C.-F. Chi, H.-W. Cho, H. Teng, C.-Y. Chuang, Y.-M. Chang, Y.-J. Hsu and Y.-L. Lee, *Appl. Phys. Lett.*, 2011, **98**, 012101.

21 K.-H. Lin, C.-Y. Chuang, Y.-Y. Lee, F.-C. Li, Y.-M. Chang, I. P. Liu, S.-C. Chou and Y.-L. Lee, *J. Phys. Chem. C*, 2011, **116**, 1550–1555.

22 S. Cheng, W. Fu, H. Yang, L. Zhang, J. Ma, H. Zhao, M. Sun and L. Yang, *J. Phys. Chem. C*, 2011, **116**, 2615–2621.

23 X. F. Gao, W. T. Sun, G. Ai and L. M. Peng, *Appl. Phys. Lett.*, 2010, **96**, 153104.

24 X. Yin, W. Que, D. Fei, H. Xie, Z. He and G. Wang, *Electrochim. Acta*, 2013, **89**, 561–570.

25 X.-Y. Yu, J.-Y. Liao, K.-Q. Qiu, D.-B. Kuang and C.-Y. Su, *ACS Nano*, 2011, **5**, 9494–9500.

26 P. K. Santra and P. V. Kamat, *J. Am. Chem. Soc.*, 2012, **134**, 2508–2511.

27 G. Rainò, I. Moreels, A. Hassinen, T. Stöferle, Z. Hens and R. F. Mahrt, *Nano Lett.*, 2012, **12**, 5224–5229.

28 K. Wu, W. E. Rodríguez-Córdoba, Z. Liu, H. Zhu and T. Lian, *ACS Nano*, 2013, **7**, 7173–7185.

29 G. Hodes, *J. Phys. Chem. C*, 2008, **112**, 17778–17787.

30 A. Kongkanand, K. Tvrdy, K. Takechi, M. Kuno and P. V. Kamat, *J. Am. Chem. Soc.*, 2008, **130**, 4007–4015.

31 N. Guijarro, T. Lana-Villarreal, Q. Shen, T. Toyoda and R. Gomez, *J. Phys. Chem. C*, 2010, **114**, 21928–21937.

32 N. Guijarro, Q. Shen, S. Gimenez, I. Mora-Sero, J. Bisquert, T. Lana-Villarreal, T. Toyoda and R. Gomez, *J. Phys. Chem. C*, 2010, **114**, 22352–22360.

33 Q. Shen, Y. Ayuzawa, K. Katayama, T. Sawada and T. Toyoda, *Appl. Phys. Lett.*, 2010, **97**, 263113.

34 S. Kuwahara, H. Hata, S. Taya, N. Maeda, Q. Shen, T. Toyoda and K. Katayama, *Phys. Chem. Chem. Phys.*, 2013, **15**, 5975–5981.

35 N. Maeda, H. Hata, N. Osada, Q. Shen, T. Toyoda, S. Kuwahara and K. Katayama, *Phys. Chem. Chem. Phys.*, 2013, **15**, 11006–11013.

36 Q. Shen and T. Toyoda, *Thin Solid Films*, 2003, **438**–439, 167–170.

37 R. Jayakrishnan, P. N. Jaya, K. Beena Annie, S. K. Kulkarni and R. K. Pandey, *Semicond. Sci. Technol.*, 1996, **11**, 116.

38 S. Gorer and G. Hodes, *J. Phys. Chem.*, 1994, **98**, 5338–5346.

39 S.-m. Yang, C.-h. Huang, J. Zhai, Z.-s. Wang and L. Jiang, *J. Mater. Chem.*, 2002, **12**, 1459–1464.

40 Y. Tachibana, H. Y. Akiyama, Y. Ohtsuka, T. Torimoto and S. Kuwabata, *Chem. Lett.*, 2007, **36**, 88–89.

41 K. Katayama, M. Yamaguchi and T. Sawada, *Appl. Phys. Lett.*, 2003, **82**, 2775–2777.

42 M. Yamaguchi, K. Katayama and T. Sawada, *Chem. Phys. Lett.*, 2003, **377**, 589–594.

43 A. Rosencwaig and A. Gersho, *J. Appl. Phys.*, 1976, **47**, 64–69.

44 S. Nomura and T. Kobayashi, *Solid State Commun.*, 1991, **78**, 677–680.

45 T. Zewdu, J. N. Clifford, J. P. Hernandez and E. Palomares, *Energy Environ. Sci.*, 2011, **4**, 4633–4638.